

Crystallographic disorder and electron scattering on structural two-level systems in

$\text{ZrAs}_{1.4}\text{Se}_{0.5}$

This article has been downloaded from IOPscience. Please scroll down to see the full text article.

2005 J. Phys.: Condens. Matter 17 5481

(<http://iopscience.iop.org/0953-8984/17/36/004>)

View [the table of contents for this issue](#), or go to the [journal homepage](#) for more

Download details:

IP Address: 129.252.86.83

The article was downloaded on 28/05/2010 at 05:54

Please note that [terms and conditions apply](#).

Crystallographic disorder and electron scattering on structural two-level systems in $\text{ZrAs}_{1.4}\text{Se}_{0.5}$

M Schmidt, T Cichorek¹, R Niewa, A Schlechte, Yu Prots, F Steglich and R Kniep

Max Planck Institute for Chemical Physics of Solids, Nöthnitzer Straße 40, 01187 Dresden, Germany

Received 19 April 2005, in final form 6 July 2005

Published 26 August 2005

Online at stacks.iop.org/JPhysCM/17/5481

Abstract

Single crystals of $\text{ZrAs}_{1.4}\text{Se}_{0.5}$ (PbFCl-type structure) were grown by chemical vapour transport. While their thermodynamic and transport properties are typical for ordinary metals, the electrical resistivity exhibits a shallow minimum at low temperatures. Application of strong magnetic fields does not influence this anomaly. The minimum of the resistivity in $\text{ZrAs}_{1.4}\text{Se}_{0.5}$ apparently originates from interaction between the conduction electrons and structural two-level systems. Significant disorder in the As–Se substructure is inferred from x-ray diffraction and electron microprobe studies.

1. Introduction

Several thermal, electrical and magnetic properties of ordinary metals in the presence of dilute magnetic impurities appear to be anomalous with respect to the properties observed in the presence of nonmagnetic impurities. For instance, the electrical resistivity $\rho(T)$ of an ordinary metal containing nonmagnetic impurities decreases monotonically with decreasing temperature and becomes constant at low temperatures. In contrast, the resistivity of a normal metal in the presence of dilute magnetic impurities exhibits a rather shallow minimum at low temperatures [1, 2]. This resistivity anomaly reflects an unusual nature of the scattering of conduction electrons from an isolated impurity spin. As originally suggested by Cochrane *et al* [3], qualitatively different scattering of conduction electrons from nonmagnetic and magnetic impurities can be lifted in metals with structural two-level systems (TLS), i.e., tunnelling defects with two energy levels. The simplest realization of a tunnelling centre is believed to be an atom that quantum-mechanically tunnels between two metastable states of the double-well potential. Indeed, under some circumstances, internal degrees of freedom of a tunnelling centre may be mapped to internal degrees of freedom of the magnetic impurity embedded in

¹ Permanent address: Institute of Low Temperature and Structure Research, Polish Academy of Sciences, 50-950 Wrocław, Poland.

the Fermi sea, and hence an additional T -dependent resistivity, being hardly affected by a strong magnetic field, may occur at low temperatures [4].

Interactions between the conduction electrons and structural TLS appear to be remarkably strong in certain arsenide selenides. For example, the resistivity of diamagnetic ThAsSe frequently displays a logarithmic correction below around 20 K, which is affected by neither strong magnetic fields nor high hydrostatic pressures [5]. The existence of tunnelling centres in single crystals of ThAsSe is reflected by, for example, a glassy-type temperature dependence of both the thermal conductivity and specific heat at $T \lesssim 1$ K [5, 6]. For UAsSe and its derivatives, a strongly sample-dependent upturn in $\rho(T)$ is observed deep in the ferromagnetic state [7]. Whereas an influence of structural TLS on the charge transport in actinide-based arsenide selenides is well established, very little is known of the nature of tunnelling centres in these materials [8, 9].

Guided by the remarkably similar physical properties of ThAsSe and UAsSe, we have grown single crystals of an isostructural Zr-based compound to verify our hypothesis on an interaction between the conduction electrons and TLS in these materials. In this paper we report on the basic physical properties of $\text{ZrAs}_{1.4}\text{Se}_{0.5}$, compare them with those of ThAsSe, and discuss some crystallochemical aspects of the As–Se substructure being indicative of structural disorder in layered arsenide selenides.

2. Experimental details

Single crystals of the ternary phase were grown by chemical vapour transport from a pre-reacted substrate. The microcrystalline powder had been synthesized by reaction of the elements (Zr 99.8% Chempur, As 99.9999% Chempur, Se 99.999% Chempur) in a molar ratio of 1:1:1. The elements were placed in an evacuated quartz ampoule and a glassy carbon crucible was used to prevent a possible reaction of zirconium with silica. The reaction was conducted by a gradual increase in temperature from 473 to 1173 K over 14 days followed by a subsequent treatment at the final temperature for 14 days more. For the crystal growth experiments, iodine (Chempur 99.999%) served as a transport agent (1 mg cm^{-3}). The deposition of crystals was realized exothermically from $T_1 = 1123$ K to $T_2 = 1223$ K over a distance of 10 cm (diameter of the ampoule: 20 mm). The as-grown crystals show metallic lustre. All presented data were obtained on one single crystal or parts of it. The specimen investigated has a size of $2 \text{ mm} \times 0.5 \text{ mm} \times 0.3 \text{ mm}$ and a mass of 2 mg (figure 1).

The chemical composition of the crystal was initially examined by scanning electron microscopy with energy dispersive x-ray microanalyses utilizing a Philips XL30 scanning electron microscope. The precise composition was determined on polished surfaces using electron-probe microanalysis. The investigations were done with a wavelength dispersive system (WDXS) Cameca SX100. Elemental standards for zirconium, arsenic and selenium were used.

The quality of the crystal was checked with Laue diffractograms. Room-temperature x-ray diffraction intensity data were collected on a STOE IPDS diffractometer using graphite monochromated $\text{Ag K}\alpha$ radiation (above the absorption threshold of the Zr K-edge). Accurate unit cell parameters were determined from the ground crystal on a STOE STADIP-MP diffractometer using $\text{Cu K}\alpha_1$ radiation after all the measurements had been performed. The structure was solved and refined with the SHELX package of programs [10, 11]. A numerical absorption correction of the intensity data was carried out for the optimized shape of the crystal by using STOE X-RED and X-SHAPE programs.

The electrical resistivity was investigated along the a axis by a conventional four-point ac method. Experiments were performed in zero and applied magnetic field of 9 T down

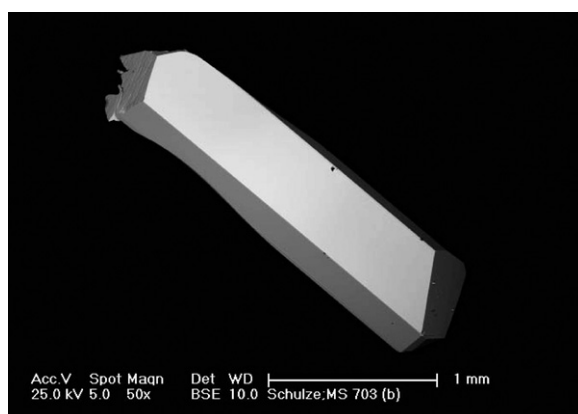


Figure 1. Single crystal of $\text{ZrAs}_{1.40}\text{Se}_{0.50}$ investigated in this work.

Table 1. Positional and displacement parameters (10^{-4} pm^2) for $\text{ZrAs}_{1.40}\text{Se}_{0.50}$. (Note: $U_{12} = U_{13} = U_{23} = 0$.)

Atom	Site	x	y	z	$U_{11} = U_{22}$	U_{33}	Occ.
Zr	2c	1/4	1/4	0.265 21(6)	0.0050(2)	0.0031(2)	1
As	2a	3/4	1/4	0	0.0111(3)	0.0034(3)	0.906(6)
Se/As	2c	1/4	1/4	0.620 99(7)	0.0044(2)	0.0041(3)	0.501(6)/0.499

to 2 K. Electrical contacts were made by spot welding $25 \mu\text{m}$ gold wires to the crystal. The heat capacity was determined with the aid of the thermal relaxation technique utilizing a commercial microcalorimeter (Quantum Design, model PPMS). The dc magnetic susceptibility was measured using a SQUID magnetometer (Quantum Design, model MPMS).

3. Results

3.1. Crystal structure and chemical composition

The single crystal diffraction data set obtained could be indexed on the basis of a tetragonal unit cell with $a = 374.17(7) \text{ pm}$, $c = 811.9(2) \text{ pm}$. A precise unit cell refinement with the Guinier technique resulted in $a = 374.69(1) \text{ pm}$, $c = 807.16(2) \text{ pm}$. The extinction conditions led to the space groups $P4/n$ and $P4/nmm$. Refinements in both space groups resulted in qualitatively identical structure models; therefore the higher symmetry space group $P4/nmm$ was chosen for the detailed structure analysis.

After an initial refinement of an ordered ZrSiS -type structure As was successively introduced on the Se site, leading to a structure model with the composition $\text{ZrAs}(\text{Se}_{0.60(1)}\text{As}_{0.40})$ and reliability factors of $R1/wR2 = 0.030/0.074$. On refinement the As site occupancy dropped to 0.906(6), while the Se/As ratio on the Se site adjusted to 0.501(6)/0.499 and the reliability factors dropped to $R1/wR2 = 0.019/0.042$ in a stable refinement. The resulting composition from x-ray diffraction analysis is $\text{ZrAs}_{0.90(1)}(\text{Se}_{0.50(1)}\text{As}_{0.50}) = \text{ZrAs}_{1.40}\text{Se}_{0.50}$ (figure 2). The anisotropic displacement parameters are nearly unaffected by these operations. This indicates an excellent structural model intensity description, which is additionally in excellent agreement with WDX analyses. Tables 1 and 2 present the structure determination and crystallographic data. A refinement of intensity data obtained with Mo $K\alpha$ radiation (below the absorption threshold of the Zr K-edge) did not allow any refinement of the As/Se ratio.

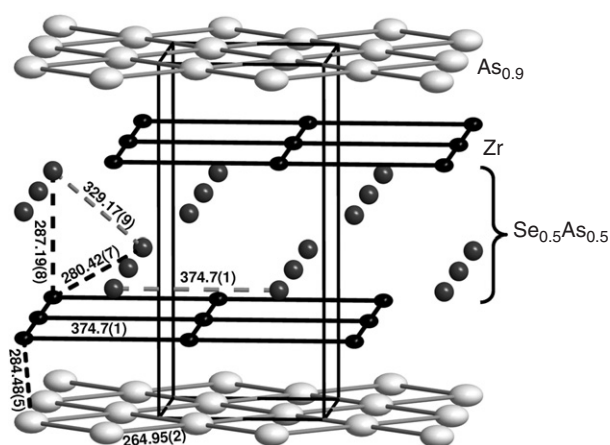


Figure 2. PbFCl-type crystal structure of $\text{ZrAs}_{0.90(1)}(\text{Se}_{0.50(1)}\text{As}_{0.50}) = \text{ZrAs}_{1.40}\text{Se}_{0.50}$. Note the 90% occupation of the As site and the anomalous displacement parameters. Distances are given in pm.

Table 2. Crystallographic data for $\text{ZrAs}_{1.40}\text{Se}_{0.50}$.

Crystal size (mm^3)	$0.035 \times 0.075 \times 0.090$
Space group	$P4/nmm$ (No. 129)
Lattice parameters (pm)	$a = 374.69(1)$ $c = 807.16(2)$
Cell volume (10^6 pm^3), Z	113.316(4), 2
Image plate distance (mm)	60
ρ range (deg), $\Delta\rho$ (deg)	200, 1
2θ range (deg)	$2\theta < 55.8$
hkl range	$-6 \leq h \leq 6$ $-6 \leq k \leq 6$ $-13 \leq l \leq 13$
No of measured reflections, R_{int}	2183, 0.038
No of independent reflections	200
No of refined parameters	12
Program	SHELX97 [11]
$R_{\text{gt}}(F)$, $R_{\text{all}}(F)$	0.019, 0.042
Goof	0.882
Extinction coefficient	0.28(1)
Largest peaks in difference electron density	0.95, -2.49
$\Delta\rho_{\text{max}}$, $\Delta\rho_{\text{min}}$ (10^{-6} pm^{-3})	

$\text{ZrAs}_{0.90(1)}(\text{Se}_{0.50(1)}\text{As}_{0.50}) = \text{ZrAs}_{1.40}\text{Se}_{0.50}$ crystallizes in the UPS branch (substitution variant of the Fe_2As -type, often referred to as ZrSiS-type) of the PbFCl-type structure characterized by a larger ratio $c/a \geq 2.0$ together with a large fractional parameter of the metal atom (Zr) $z \geq 2.2$ as compared to the BiOI-type [12]. In this structure type typically the larger anions occupy the 2c site and the smaller anions the 2a site. Both anion sites might be susceptible to substitution with the respective other species or a third element with the restriction of atomic/ionic radii fit [13]. For the ZrSiS branch of MXY compounds appreciable X–X bonding in the densely packed quadratic layer of X is commonly discussed, while Y–Y bonding is typically moderate.

Refinements of As/Se ratios based on x-ray diffraction data present a problem due to the difference of only one electron for those elements. Additionally, a scaling problem for refinement of the As-site occupation arises. Still, the obtained data are in excellent agreement with the WDX analysis results ($\text{ZrAs}_{1.40(1)}\text{Se}_{0.50(1)}$ versus 34.69(4) at.% Zr, 48.51(5) at.% As,

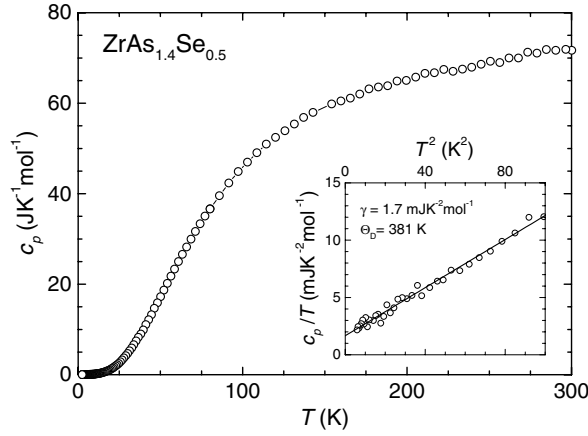


Figure 3. Temperature dependence of the heat capacity for a single crystal of $\text{ZrAs}_{1.4}\text{Se}_{0.5}$. Inset: the low-temperature specific heat, as c_p/T versus T^2 , between 1.8 and 10 K. The solid curve represents a $\gamma T + \beta T^3$ dependence with $\beta = 3 \times 1944/\Theta_D^3$ in units of $\text{J K}^{-4} \text{mol}^{-1}$ and we have neglected defects in the 2a anionic site.

and 16.80(3) at. % Se, i.e., $\text{ZrAs}_{1.398}\text{Se}_{0.484}$) for the identical crystal, supporting the composition and crystallographic disorder model. For the As-rich phase in the system Zr–As–Se, disorder with mixed occupation of the 2c site by Se and As was earlier discussed by Barthelat *et al* [14, 15], leading to a composition of $\text{ZrAs}_{0.78}(\text{As}_{0.37}\text{Se}_{0.58}) = \text{ZrAs}_{1.15}\text{Se}_{0.58}$.

3.2. Physical properties

The temperature dependence of the specific heat $c_p(T)$ of the $\text{ZrAs}_{1.4}\text{Se}_{0.5}$ single crystal is depicted in figure 3. The heat-capacity examination has not shown any phase transition. The low-temperature $c_p(T)$ data are presented as c_p/T versus T^2 in the inset of figure 3. From the straight line found for $T \leq 9$ K one obtains the Sommerfeld coefficient $\gamma = 1.7(\pm 0.2) \text{ mJ K}^{-2} \text{mol}^{-1}$ and the slope $\beta = 1.05(\pm 0.03) \times 10^{-4} \text{ J K}^{-4} \text{mol}^{-1}$, which yields a Debye temperature $\Theta_D = 381$ K.

The absence of any phase transition is also inferred from the magnetic susceptibility χ of $\text{ZrAs}_{1.4}\text{Se}_{0.5}$, which is hardly temperature dependent and negative in the temperature range 2–300 K, i.e., typical for a diamagnetic material. At 300 K and in a field of 4 T applied along the a axis, a magnetic susceptibility of $-5.5 \times 10^{-4} \text{ emu g}^{-1}$ was found. Unfortunately, the small mass of the crystal prevented us from a more detailed study of $\chi(T)$ in lower fields.

The temperature dependence of the electrical resistivity of $\text{ZrAs}_{1.4}\text{Se}_{0.5}$ shows a well-defined metallic behaviour, as presented in figure 4. Indeed, the $\rho(T)$ data along the a axis can be described by a generalized Bloch–Grüneisen–Mott relation with power $n = 3$ [16]:

$$\rho(T) = \rho_0 + C \left(\frac{T}{\Theta_D^R} \right)^n \int_0^{\Theta_D^R/T} \frac{x^n dx}{(e^x - 1)(1 - e^{-x})} + K T^3 \quad (1)$$

where ρ_0 is the residual resistivity, the second term represents electron–phonon scattering, and the $K T^3$ term is a correction due to s – d interband electron scattering. A least squares fit (solid line in figure 4) yields the values $\rho_0 = 140 \mu\Omega \text{ cm}$, $\Theta_D^R = 303$ K, $C = 54.5 \mu\Omega \text{ cm}$, and $K = -1.77 \times 10^{-7} \mu\Omega \text{ cm K}^{-3}$.

However, a closer inspection of our low-temperature $\rho(T)$ results for $\text{ZrAs}_{1.4}\text{Se}_{0.5}$ reveals an additional resistivity. Remarkably, this extra T -dependent term is not influenced by strong

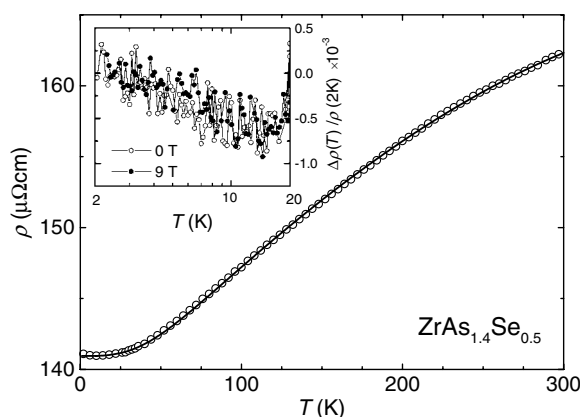


Figure 4. The electrical resistivity for a single crystal of $\text{ZrAs}_{1.4}\text{Se}_{0.5}$ as a function of temperature. The solid line is a fit as described in the text. Inset: the relative change of the low-temperature resistivity normalized to the corresponding value at 2 K obtained in zero field and 9 T.

magnetic fields. Details are depicted in the inset of figure 4. Here we have plotted the relative change of the resistivity normalized to the corresponding value at 2 K obtained in $B = 0$ and 9 T. It is noticeable that the very similar correction to the low- T resistivity has been detected in an overwhelming majority of the Zr–As–Se single crystals.

4. Discussion and conclusions

Diamagnetic $\text{ZrAs}_{1.4}\text{Se}_{0.5}$ exhibits features typical of an ordinary metal. The observed value of the Sommerfeld coefficient $\gamma = 1.7(\pm 0.2) \text{ mJ K}^{-2} \text{ mol}^{-1}$ is comparable to the electronic term in the specific heat of such metallic elements as In, Sn or Hg. On the other hand, the residual resistivity ratio as small as 1.15 resembles some alloys (e.g., manganin) rather than pure metals, and may be treated as an approximate indicator of significant disorder in the $\text{ZrAs}_{1.4}\text{Se}_{0.5}$ crystals. This is further suggested by a large value of $\rho_0 = 140 \mu\Omega \text{ cm}$. More importantly, however, a significant disorder in our samples is directly inferred from the results of both the electron-probe microanalysis and the x-ray diffraction studies. In fact, since any deviation from the 1:1:1 stoichiometry of the system crystallizing in the PbFCl-type structure always results in structural disorder, the number of imperfections has to be large in specimens with the chemical composition of 1:1.4:0.5. This general information is resolved by the results of the structure refinement, being indicative of one anionic site showing mixed occupancy of 50% As and 50% Se, and 10% of As defects on the second anionic site.

A minimum resistivity at around 12 K is the most intriguing physical property of $\text{ZrAs}_{1.4}\text{Se}_{0.5}$. In fact, since virtually the same $\Delta\rho(T)/\rho(2 \text{ K})$ data were obtained at both $B = 0$ and 9 T, a magnetic Kondo effect is very unlikely in this material². Furthermore, a field-independent upturn cannot be attributed to weak localization because this phenomenon is also highly sensitive to magnetic fields [17, 18]. For a similar reason, interaction between electrons of antiparallel momenta are apparently not responsible for the low- T anomaly. Finally, electron–electron interaction in the particle–hole diffusion channel (electrons of parallel momenta) seems to be absent in $\text{ZrAs}_{1.4}\text{Se}_{0.5}$ as well, since no obvious difference

² The most convincing proof that possible magnetic impurities are not the cause of the low- T upturn in the electrical resistivity of $\text{ZrAs}_{1.4}\text{Se}_{0.5}$ would be reflected by $\chi(T)$ and $\rho(T)$ results on the same specimen, as discussed for example for ThAsSe in [5]. Due to the small mass of our $\text{ZrAs}_{1.4}\text{Se}_{0.5}$ single crystal we could not perform such a decisive experiment.

between the zero-field and $B = 9$ T data was found at the lowest temperatures measured. Indeed, it is expected that an additional resistivity due to interactions in the diffusion channel is cut off for $g\mu_B H$ greater than $k_B T$ [17]. Forthcoming experiments at millikelvin temperatures and in higher magnetic fields should clarify to what extent this type of quantum correction influences the charge transport in Zr-based arsenide selenides.

On the other hand, a nonmagnetic anomaly of similar amplitude has been observed in all the single crystals of the related system ThAsSe. In this material electron scattering on magnetic impurities as well as quantum corrections have been unambiguously ruled out [5, 6]. Therefore, the striking similarity in the low- T behaviour of $\rho(T)$ for ThAsSe and $\text{ZrAs}_{1.4}\text{Se}_{0.5}$ allows us to consider the same origin of an electron scattering in both arsenide selenides that we relate to a presence of tunnelling centres in the As–Se substructure. Indeed, although the interatomic distances between the $2c$ sites are comparably large, arsenic and selenium atoms may be involved in a homopolar-to-heteropolar bond transformation, as discussed for As_2Se_3 [19] and As_2S_3 [20]. Such a possibility is also plausible for ThAsSe, since in some specimens of this system a large As/Se $\simeq 1.5$ content ratio was recently observed [21].

In contrast to $\text{ZrAs}_{1.4}\text{Se}_{0.5}$, the Th-based compound displays a negative temperature coefficient of the ab -plane resistivity at temperatures higher than 65 K. (The same holds true for UAsSe in the paramagnetic state.) As speculated in [22], this high-temperature increase of $\rho(T)$ may be caused by a gradual formation of covalently bonded dimers $(\text{As–As})^{4-}$ that influences the electronic structure. This scenario, being based on quite a general tendency of As ions towards homoatomic bonding in the quadratic net, was recently supported by the results of electron diffraction in ThAsSe [23]. An As–As dimerization is, to a certain extent, also possible in $\text{ZrAs}_{1.4}\text{Se}_{0.5}$, although its influence on the charge transport is not observed (cf figure 3). In fact, enhanced displacement parameters $U_{11} = U_{22} \gg U_{33}$ for As, listed in table 1, indicate the formation of As–As covalent bonds leading to diverse possible As_n anionic species and thus to static displacement from the ideal As position in favour of dynamic vibration. Average As–As distances for the ideal crystallographic position in the quadratic net from the structure refinement are $d(\text{As–As}) = 264.95(1)$ pm. For comparison, in the grey modification of arsenic, As has three nearest neighbours at 252 pm and three further neighbours at 312 pm [24]. As_4 molecules in the gas phase exhibit a distance of 243.5 pm [25]. For the As species within the $2c$ site disordered with Se species such formation of dimers or larger units As_n is unlikely, due to the considerably longer distance of $d(\text{As–As}) \geq 329$ pm in $\text{ZrAs}_{1.40(1)}\text{Se}_{0.50(1)}$.

Though the formation of covalently bonded units frequently occurs in pnictide chalcogenides crystallizing in the layered PbFCl-type structure, its direct impact on excitations of the electron gas in metallic arsenide selenides at $T \lesssim 20$ K is dubious because, first, an $(\text{As–As})^{4-}$ dimerization is already completed at much higher temperatures, as inferred from virtually identical electron diffraction patterns at 30 and 100 K in ThAsSe [23]. Second, the dimerization shows a marked sensitivity to the interatomic distances, being easily influenced by an external pressure. However, the application of high pressure alters the resistivity of ThAsSe only at high temperatures: at 1.88 GPa the maximum of the resistivity at 65 K is suppressed, whereas the low- T term is completely unchanged [5]. Finally, $\text{ZrAs}_{1.4}\text{Se}_{0.5}$ and ThAsSe show *qualitatively* different $\rho(T)$ dependences at higher temperatures, although in both diamagnets remarkably similar low- T anomalies in the electrical resistivity are observed. Nevertheless, it is conceivable that some low-energy excitations of singular $(\text{As–As})^{4-}$ dimers (but not dimerization itself) create tunnelling centres, being responsible for the shallow minimum in $\rho(T)$ of both arsenide selenides at low temperatures.

As far as the high-temperature $\rho(T)$ data for $\text{ZrAs}_{1.4}\text{Se}_{0.5}$ are concerned, a well-defined metallic character of the resistivity for a ThPS system should be quoted [26]. The ferromagnetic

UPS counterpart shows all the features characteristic of UAsSe, i.e., a strongly sample-dependent upturn in $\rho(T)$ deep in the ferromagnetic state and a negative temperature coefficient of the resistivity in the paramagnetic state [7]. However, no low- T increase of $\rho(T)$ was detected in any of the various ThPS samples so far [26].

To summarize, we have investigated one single crystal of metallic $\text{ZrAs}_{1.40}\text{Se}_{0.50}$ which shows a significant atomic disorder in the As–Se substructure. At temperatures below 12 K, $\text{ZrAs}_{1.40}\text{Se}_{0.50}$ displays an unusual, magnetic field-independent increase of the electrical resistivity upon cooling. Since a remarkably similar correction to low-temperature $\rho(T)$ has been observed in the related diamagnet ThAsSe, an anomalous scattering mechanism in the isostructural Zr-based system appears to be also caused by nonmagnetic interactions between the conduction electrons and structural two-level systems. The results of x-ray diffraction and electron microprobe investigations show that a formation of tunnelling centres might be triggered off by empty places in the As ($2a$) layers or/and the mixed occupation of the $2c$ sites by arsenic and selenium.

Acknowledgments

We would like to thank U Burkhardt and K Schulze for their help with WDX, and R Cardoso-Gil for assistance with powder x-ray diffraction. We also want to thank W Schnelle for a critical reading of the manuscript.

References

- [1] Meissner W and Voigt G 1930 *Ann. Phys.* **7** 761
Meissner W and Voigt G 1930 *Ann. Phys.* **7** 892
- [2] Kondo J 1964 *Solid State Phys.* **89** 10
- [3] Cochrane R W, Harris R, Strom-Olsen J O and Zuckerman M J 1975 *Phys. Rev. Lett.* **35** 676
- [4] See, for a review Cox D L and Zawadowski A 1998 *Adv. Phys.* **47** 599
- [5] Cichorek T, Aoki H, Custers J, Gegenwart P, Steglich F, Henkie Z, Bauer E D and Maple M B 2003 *Phys. Rev. B* **68** 144411
- [6] Cichorek T, Sanchez A, Gegenwart P, Wojakowski A, Henkie Z, Auffermann G, Weickert F, Paschen S, Kniep R and Steglich F 2005 *Phys. Rev. Lett.* **94** 236603
- [7] Cichorek T, Wawryk R, Wojakowski A, Henkie Z and Steglich F 2003 *Acta Phys. Pol. B* **34** 1339
- [8] Henkie Z, Cichorek T, Pietraszko A, Fabrowski R, Wojakowski A, Kuzhel B S, Kępiński L, Krajczyk L, Gukasov A and Wiśniewski P 1998 *J. Phys. Chem Solids* **59** 38
- [9] Henkie Z, Pietraszko A, Wojakowski A, Kępiński L and Cichorek T 2001 *J. Alloys Compounds* **317/318** 52
- [10] Sheldrick G, Krüger C and Goddard R 1985 *SHELXS-97 Göttingen, Germany*
- [11] Sheldrick G 1997 *SHELXL97-2, Göttingen, Germany*
- [12] Flahaut J 1974 *J. Solid State Chem.* **9** 124
- [13] Wang C and Hughbanks T 1995 *Inorg. Chem.* **34** 5524
- [14] Barthelat J C and Jeannin Y 1972 *J. Less-Common Met.* **26** 273
- [15] Barthelat J C, Jeannin Y and Rancurel J F 1969 *C. R. Acad. Sci. Paris* **268** 1756
- [16] Grimvall G 1986 *Thermophysical Properties of Materials* (Amsterdam: North-Holland) p 218
- [17] Lee P A and Ramakrishnan T V 1985 *Rev. Mod. Phys.* **57** 287
- [18] Monsterleet J M, Capoen B and Biskupski G 1997 *J. Phys.: Condens. Matter* **9** 8657
- [19] Li J and Drabold A D 2000 *Phys. Rev. Lett.* **85** 2785
- [20] Uchino T and Elliot S R 2003 *Phys. Rev. B* **67** 174201
- [21] Burkhardt U, private communication
- [22] Schoenes J, Bacsá W and Hulliger F 1988 *Solid State Commun.* **68** 287
- [23] Withers R L, Vincent R and Schoenes J 2004 *J. Solid State Chem.* **177** 701
- [24] Schiferl D and Barrett C S 1969 *J. Appl. Crystallogr.* **2** 30
- [25] Morino Y, Ukaii T and Ito T 1966 *Bull. Chem. Soc. Japan* **39** 64
- [26] Wawryk R, Wojakowski A, Pietraszko A and Henkie Z 2005 *Solid State Commun.* **133** 295